3653

TECH LIBRARY KAFB, NM
0065065

NATIONAL ADVISORY COMMITTEE FOR AERONAUTICS

TECHNICAL NOTE 2235

THE BOUNDARY-LAYER AND STALLING CHARACTERISTICS OF THE NACA 64A010 AIRFOIL SECTION

By Robert F. Peterson

Ames Aeronautical Laboratory
Moffett Field, Calif.

Washington
November 1950

AFMDC
TECH[illegible]
[illegible]

TECH LIBRARY KAFB, NM

0065065

NATIONAL ADVISORY COMMITTEE FOR AERONAUTICS

TECHNICAL NOTE 2235

THE BOUNDARY-LAYER AND STALLING CHARACTERISTICS OF THE NACA 64A010 AIRFOIL SECTION

By Robert F. Peterson

SUMMARY

A wind-tunnel investigation of the NACA 64A010 airfoil section was conducted to determine the boundary-layer and stalling characteristics at low speed. The tests were made at a Reynolds number of 4.1 million and included force measurements, pressure-distribution measurements, flow studies by the liquid-film technique, and boundary-layer measurements.

A small region of separated flow was evident, near the leading edge on the upper surface of the airfoil at positive angles of attack; this region moved forward and became narrower as the angle of attack was increased. At an angle of attack of 9.5° the separated flow failed to reattach to the surface, causing the stall. Since there was no turbulent separation at the trailing edge, the lift-curve peak was sharp and the stall occurred suddenly and with no warning.

INTRODUCTION

An investigation of the boundary-layer and stalling characteristics of the NACA 64A010 airfoil section was undertaken in the Ames 7- by 10-foot wind-tunnel No. 1 because this section, with other thin airfoil sections of the NACA 63- and 64-series, is currently being widely considered for use on high-speed and swept-wing aircraft, and specific knowledge of the flow associated with this section would be particularly valuable.

Investigations of the boundary-layer and stalling characteristics of the NACA 63_1-012, 63-009, and 64A006 airfoil sections have been reported in references 1, 2, and 3, respectively. The stalls of both the NACA 63_1-012 and the NACA 63-009 airfoil sections were very abrupt and occurred when the separated boundary layer near the leading edge failed to reattach to the surface of the airfoil. The NACA 64A006 section had a well-rounded lift-curve peak because the stall was caused by a gradual chordwise growth from the leading edge of the region of separated flow over the upper surface. With the NACA 64A006 section, $c_{l_{max}}$ was obtained when the point of reattachment of the separated flow was near the trailing edge of the airfoil.

This report contains the results of the measurements of the aerodynamic forces and moments, chordwise distributions of pressure, and velocities within the boundary layer. Studies of the flow patterns near the leading edge were also made by a technique employing a thin film of liquid applied to the surface. All tests were conducted at a Reynolds number of 4.1 million and a Mach number of 0.167.

NOTATION

c	wing chord, feet
c_d	section drag coefficient $\left(\frac{D}{q_o c}\right)$
c_l	section lift coefficient $\left(\frac{L}{q_o c}\right)$
c_m	section pitching-moment coefficient referred to the quarter-chord point $\left(\frac{M}{q_o c^2}\right)$
D	drag per unit span, pounds
H_o	free-stream total pressure, pounds per square foot
L	lift per unit span, pounds
M	pitching moment per unit span, pound-feet
p	local static pressure, pounds per square foot
q_o	free-stream dynamic pressure, pounds per square foot
S	pressure coefficient $\left(\frac{H_o - p}{q_o}\right)$
u	local velocity inside boundary layer, feet per second
U	local velocity outside boundary layer, feet per second
x	distance from airfoil leading edge parallel to chord line, feet
y	distance above airfoil surface, feet
α	angle of attack, degrees

MODEL

The model was built with an NACA 64A010 airfoil section, a 3-1/2-foot chord (see reference 4 for ordinates), and a plain, 30-percent-chord, trailing-edge flap. For the purposes of this test, the flap was completely sealed and was not deflected.

Circular plates, 6 feet in diameter, were attached to each end of the model and formed a part of the tunnel floor and ceiling.

At the midspan section of the model, a row of flush orifices was provided for obtaining the chordwise pressure-distribution data. The model is shown mounted in the wind tunnel in figure 1.

TESTS AND APPARATUS

The wind-tunnel balance system was used to measure the lift, drag, and pitching moment. Surface pressure data were obtained by photographing manometers connected to the orifices.

The liquid-film technique, as described in reference 2, was used to indicate the characteristics of the boundary layer near the leading edge and to permit measurement of the chordwise extent of the separated flow in this region. The measurements were made from the leading edge of the model, parallel to the chord line.

The boundary-layer data were obtained with small pressure-sensing rakes attached to the surface of the model. The total-pressure tubes used in the boundary-layer survey rakes were of stainless steel with a wall thickness of 0.0025 inch, flattened so that the opening perpendicular to the surface of the airfoil was 0.002 inch. The center line of the tube on the surface of the model was therefore 0.0035 inch above the surface, precluding measurements of the true total pressure at the surface. Measurements of the surface static pressure by the flush orifices in the model were supplemented by additional measurements with a movable static-pressure tube on the surface of the model.

RESULTS AND DISCUSSION

None of the data of the present report has been corrected for wind-tunnel-wall effects because these corrections could have been applied only to part of the data. Corrections to boundary-layer data, such as velocity-profile measurements, are not available. Furthermore, the corrections to the force and the pressure-distribution data are not of a nature to affect the significance of the conclusions drawn.[1]

Force and Moment Characteristics

The lift, drag, and pitching-moment characteristics are shown in figure 2. As can be seen from the curves of section lift coefficient versus angle of attack, the stall was very sudden and occurred with no detectable warning. It is to be noticed that the maximum value of the section lift coefficient obtained from integrating the pressure distribution is higher than that for the force-measurement curve. The flow at the center of the model, where the pressure orifices were, was smooth at high angles of attack, but at the ends of the model the flow was disturbed by the boundary layer of the tunnel floor and ceiling. This disturbance caused a loss of lift at the ends of the model at high angles of attack, and since the value indicated by the balance system was an average lift for the whole wing, it was naturally less at the maximum lift coefficient than was shown by the pressure distribution.

The drag curves also show differences in the values of the coefficients obtained by the two methods. The drag obtained from the pressure distributions does not contain the drag due to the end plates, nor does it contain the skin friction, both of which are included in the data obtained from the force measurements.

The pitching-moment curves obtained by the two methods agree within experimental accuracy and have the same form.

Pressure Distributions

The chordwise variation of the pressure coefficient S for various values of the lift coefficient is given in figure 3. These pressure coefficients are the uncorrected, observed values. The peak-pressure coefficients grew uniformly with increasing angle of attack until the maximum section lift coefficient of 1.07 was attained ($\alpha = 9.5^\circ$). When the airfoil stalled, the pressure peak collapsed and a region of approximately constant pressure formed over the nose of the airfoil, extending back to 15-percent chord, after which there was a partial pressure recovery, although free-stream static pressure was not regained at the trailing edge.

---

[1] Corrected aerodynamic data for the NACA 64A010 section may be obtained from reference 4.

Figure 4 shows the pressure coefficients plotted against angle of attack for given chordwise stations. The small discontinuities in the curves are caused by the presence of a small "bubble" of separated flow near the leading edge. In reference 2, this phenomenon of separation and reattachment is explained in detail.

Liquid-Film Studies

Figure 5 shows the variation in location and extent of the region of separated flow as determined by the liquid-film method for both the NACA 64A010 airfoil section and the NACA 63-009 airfoil section from reference 2. These data agree qualitatively up to a value of the lift coefficient ($c_l = 0.99$) just prior to the stall. This is to be expected inasmuch as the ordinates of the two airfoils agree within two-tenths of 1 percent at the 10-percent-chord station, and the difference between the two sections ahead of this station decreases. Furthermore, the leading-edge radii are 0.631- and 0.687-percent chord for the NACA 63-009 and NACA 64A010 airfoils, respectively.

In comparing the data from reference 2 with that of the present report (fig. 5), it should be borne in mind that the two tests were conducted at different Reynolds numbers and, as is pointed out in reference 2, the chordwise extent of the bubble should increase with decreasing Reynolds number.

For the NACA 64A010 airfoil at a value of the lift coefficient of 0.99, there were two separate and distinct bands of frothy liquid, with a moist area between them. The airfoil surface immediately behind the second band appeared relatively dry. These two frothy regions have been previously observed on an NACA 64A010 airfoil with the liquid-film method. The factors that cause them are not as yet understood, although it is believed that the front and rear bands define separation and reattachment, respectively.

Due to slight irregularities in the surface of the model, the chordwise extent of the region of separated flow was not uniform across the span. Therefore, each test condition was repeated, and the distances of the points of separation and reattachment from the leading edge were measured at several randomly selected spanwise stations. Figure 5 shows the average of the values as a solid line with the symbols showing the extreme conditions.

Boundary-Layer Measurements

Boundary-layer-velocity profiles were measured from 5-percent to 90-percent chord, covering the complete lift range at each of the stations. No separation of the turbulent boundary layer near the trailing edge was observed, giving additional proof to the belief that the stall was caused by failure of the separated boundary layer near the leading edge to reattach to the surface. Figure 6 presents the boundary-layer-velocity profiles for 80-percent chord, showing that the boundary layer was attached up to and including the maximum lift coefficient. Since all the boundary-layer-velocity profiles were similar to these, no others have been included.

Total-pressure measurements were made along the surface with a flattened tube as far forward as 1/8-percent chord, and the velocities calculated therefrom, using appropriate static pressures, are presented in figure 7 as surface-velocity ratio u/U. Where the surface-velocity ratio was zero, the flow was considered to be separated from the surface. The true point of separation was slightly ahead of where it is shown in figure 7 because the pressure measured by the surface tube was the average pressure between 0.0025 and 0.0045 inch from the surface. In view of the size of the tube, it is probable that there were regions of separated flow at low angles of attack which were too thin to be detected. The data of figure 7 for an angle of attack of 4° do not contain a value of $u/U = 0$. However, the trends of the curve in comparison with those for higher angles of attack indicate that a region of separation may have been present behind $x/c = 0.012$. This is further corroborated by the results presented in figure 4. For angles of attack greater than 4°, the separated region was clearly evident; it moved forward and became narrower with increasing angle of attack. The double-ended arrows in figure 7 are for the purpose of identifying the curves on opposite sides of the region of separated flow, although they do give an indication of the size and location of the separated bubble. The curve for an angle of attack of 9° is shown only in front of the region of separated flow (to $x/c = 0.005$), and does not reappear because the presence of the velocity-measuring tubes on the surface of the model near the leading edge caused the stall to occur at an angle of attack of 9°.

CONCLUSIONS

The investigation of the boundary-layer and stalling characteristics of the NACA 64A010 airfoil section indicated the following:

1. A small region of separated flow was evident on the upper surface of the airfoil at approximately 1.2-percent chord at an angle of attack of 5°. For an angle of attack of 9°, the separated region had moved forward to 0.4-percent chord and had become narrower. At an angle of attack of 9.5° the flow failed to reattach to the surface, causing the airfoil to stall very suddenly with no warning. This type of stall gives a sharp peak to the lift curve with little change of slope of the curve prior to the stall.

2. The pressure coefficient at the leading edge increased uniformly with increasing angle of attack, and the sudden and complete collapse of the pressure peak at the stall was similar to that observed on the 9- and 12-percent-thick sections of the NACA 63-series airfoils.

Ames Aeronautical Laboratory,
National Advisory Committee for Aeronautics,
Moffett Field, Calif., Sept. 26, 1950.

REFERENCES

1. McCullough, George B., and Gault, Donald E.: An Experimental Investigation of an NACA 63_1-012 Airfoil Section with Leading-Edge Suction Slots. NACA TN 1683, 1948.
2. Gault, Donald E.: Boundary-Layer and Stalling Characteristics of the NACA 63-009 Airfoil Section. NACA TN 1894, 1949.
3. McCullough, George B., and Gault, Donald E.: Boundary-Layer and Stalling Characteristics of the NACA 64A006 Airfoil Section. NACA TN 1923, 1949.
4. Loftin, Laurence K., Jr.: Theoretical and Experimental Data for a Number of NACA 6A-Series Airfoil Sections. NACA Rep. 903, 1948.

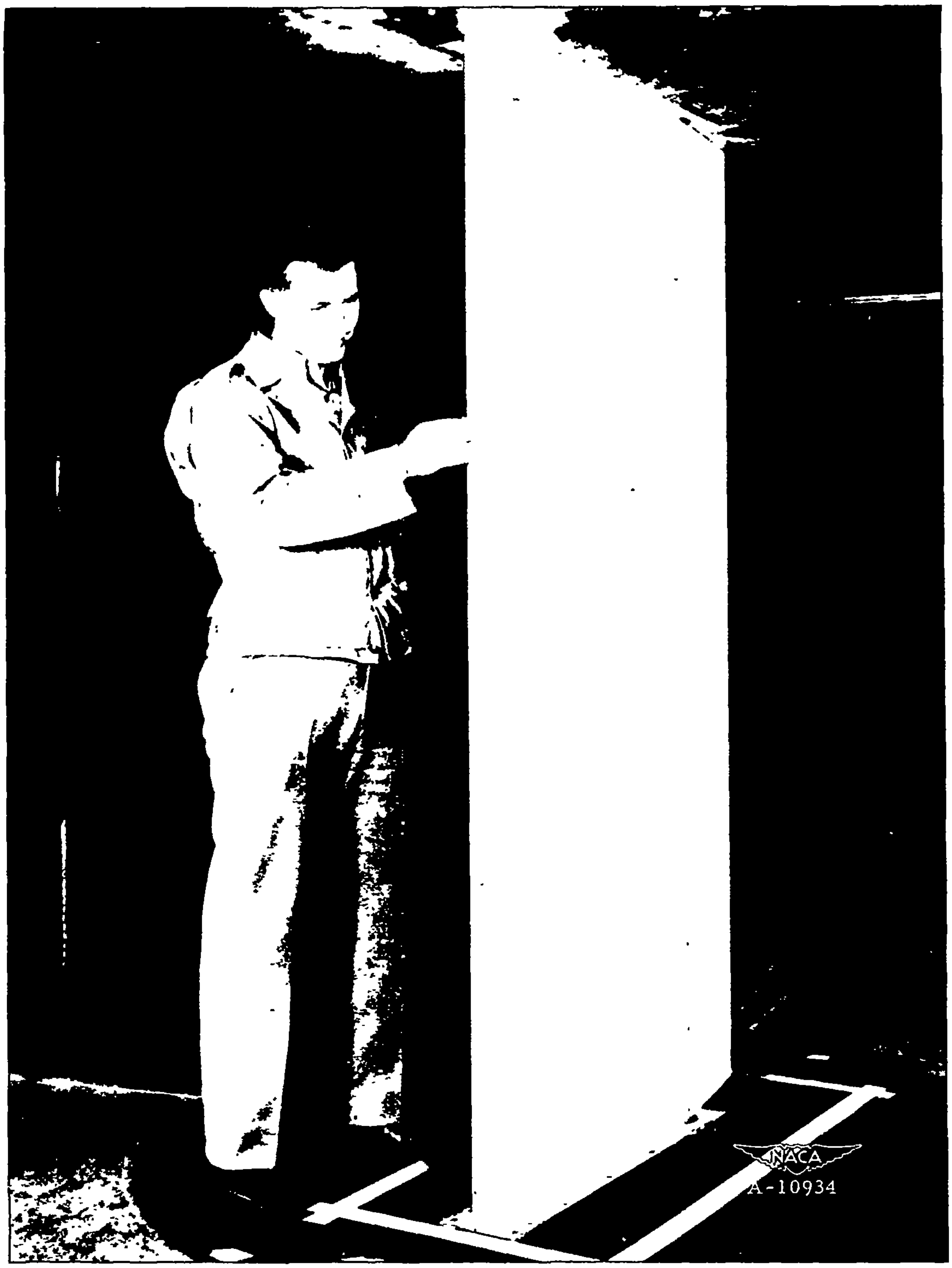
NACA
A-10934

Figure 1.– The NACA 64A010 airfoil mounted in the Ames 7- by 10-foot wind tunnel No. 1.

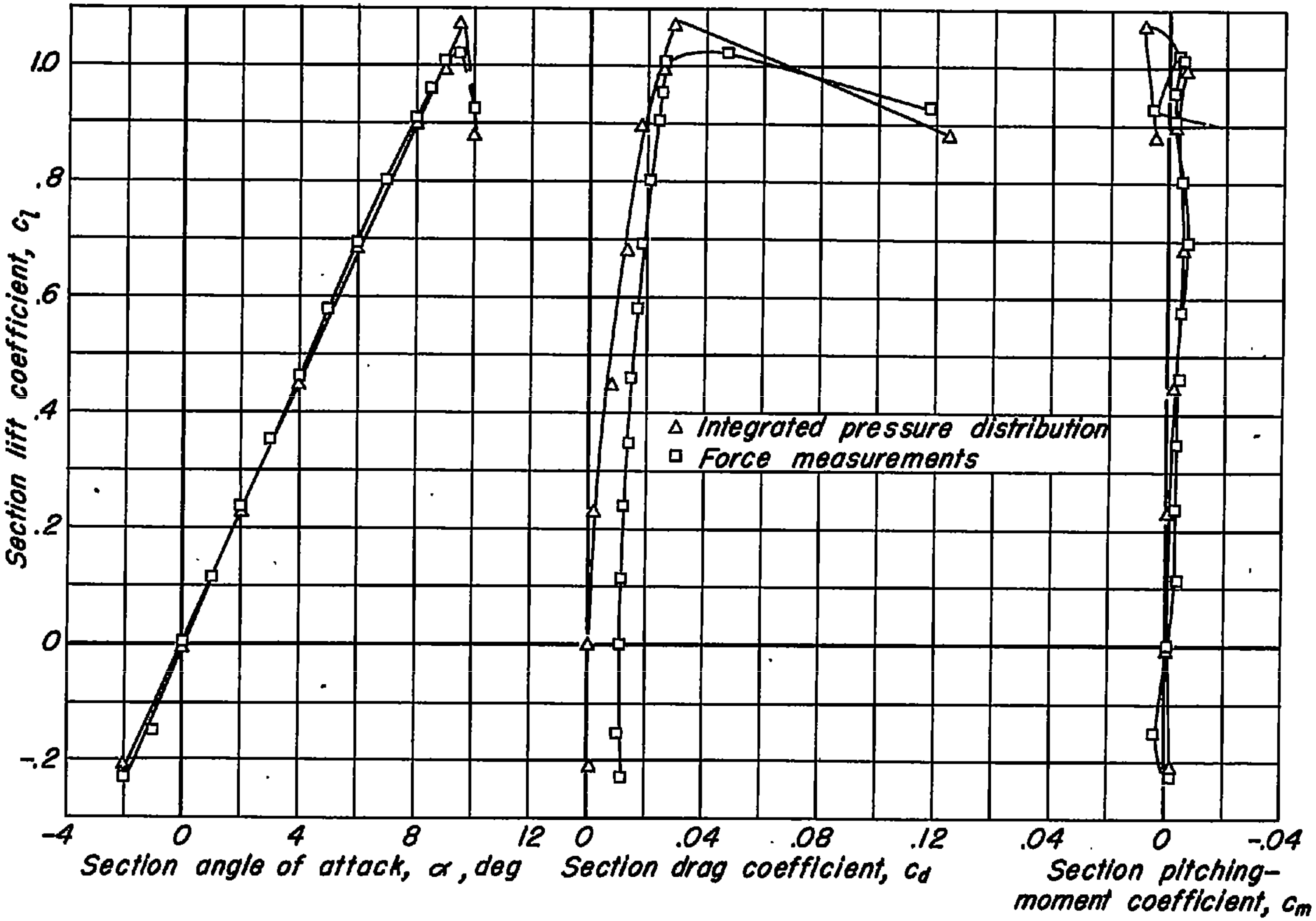

Figure 2.- Lift, drag, and pitching-moment characteristics.

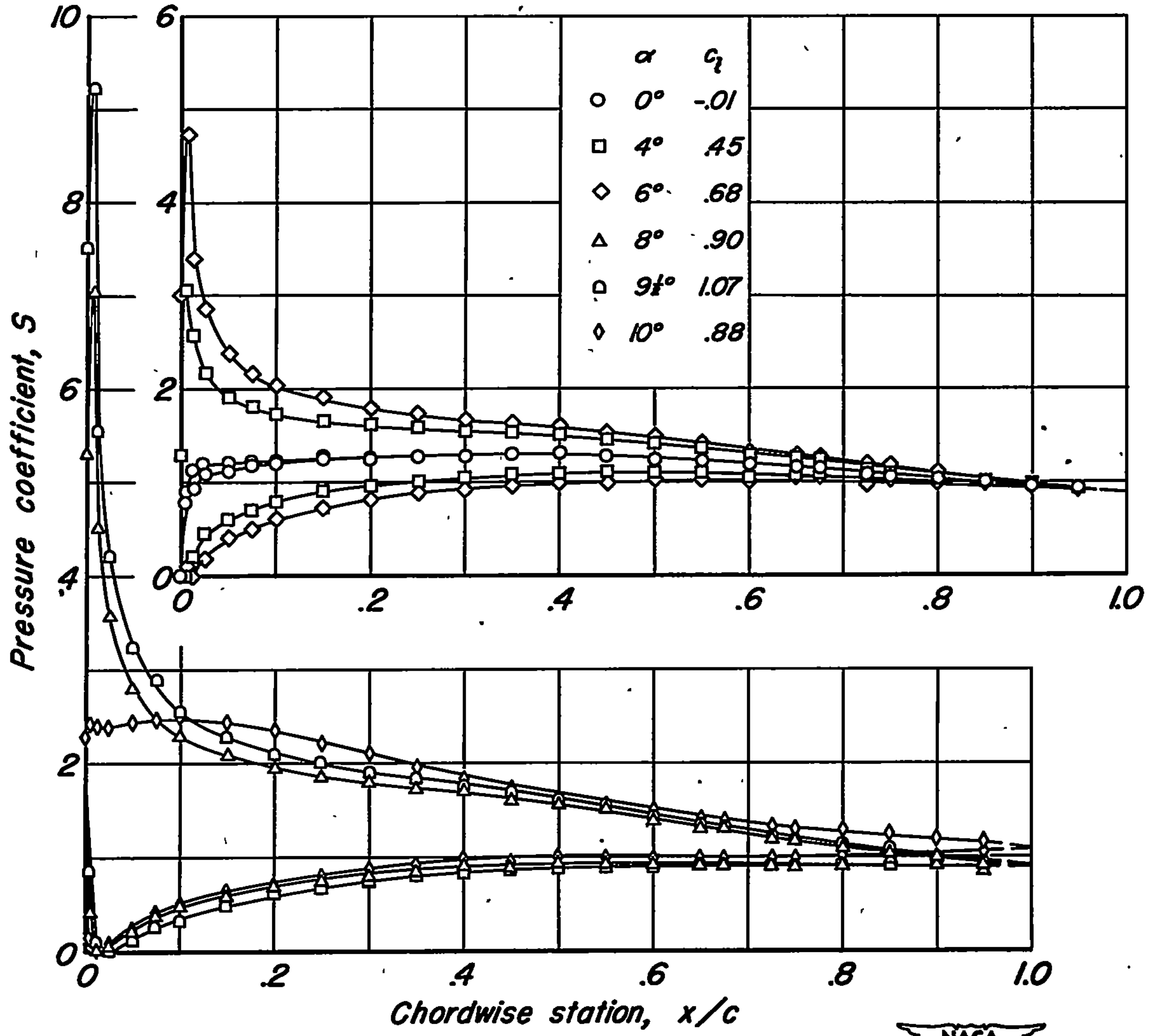

Figure 3.- Chordwise distribution of pressure.

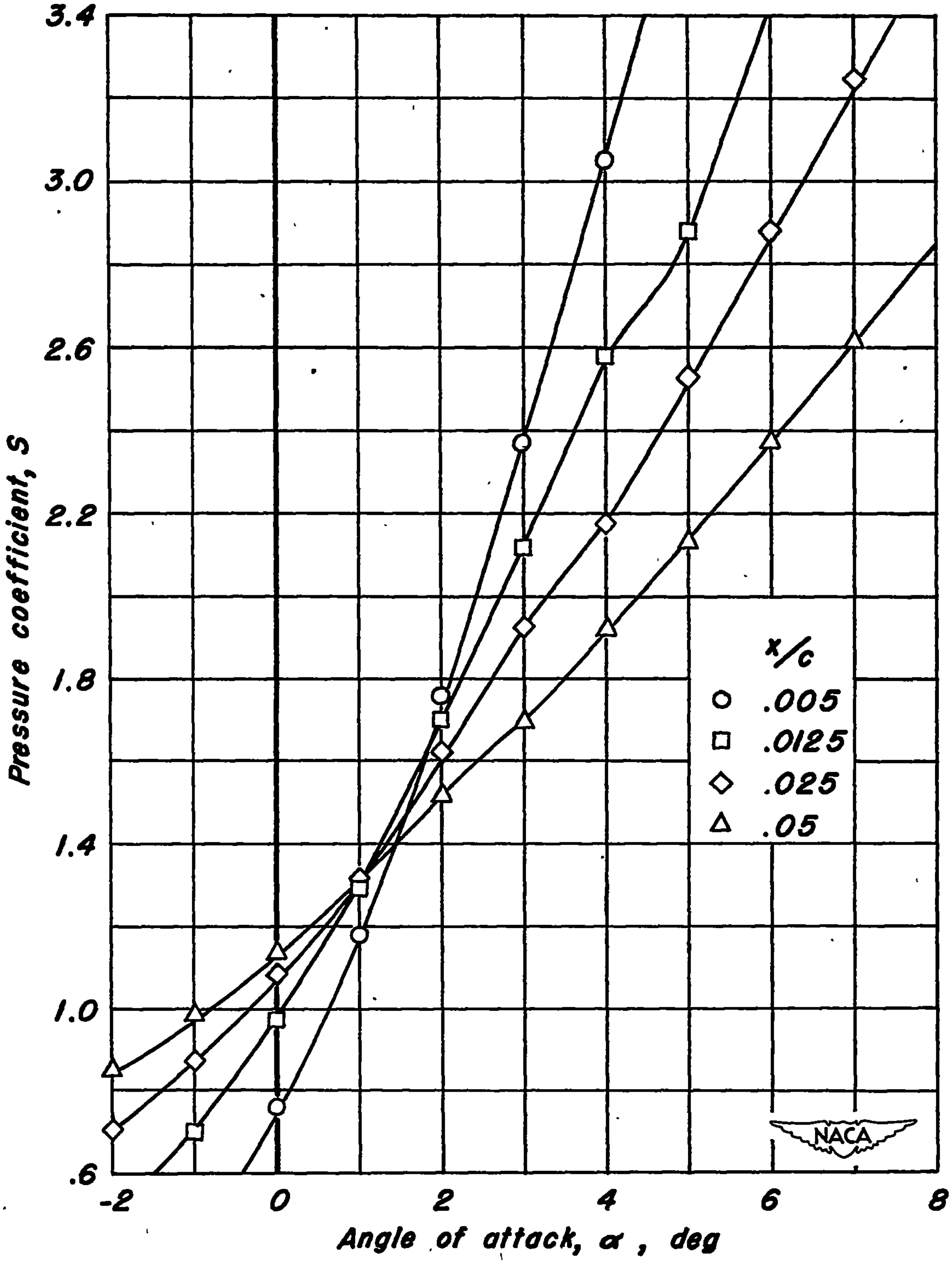

Figure 4.— Variation of pressure coefficient with angle of attack.

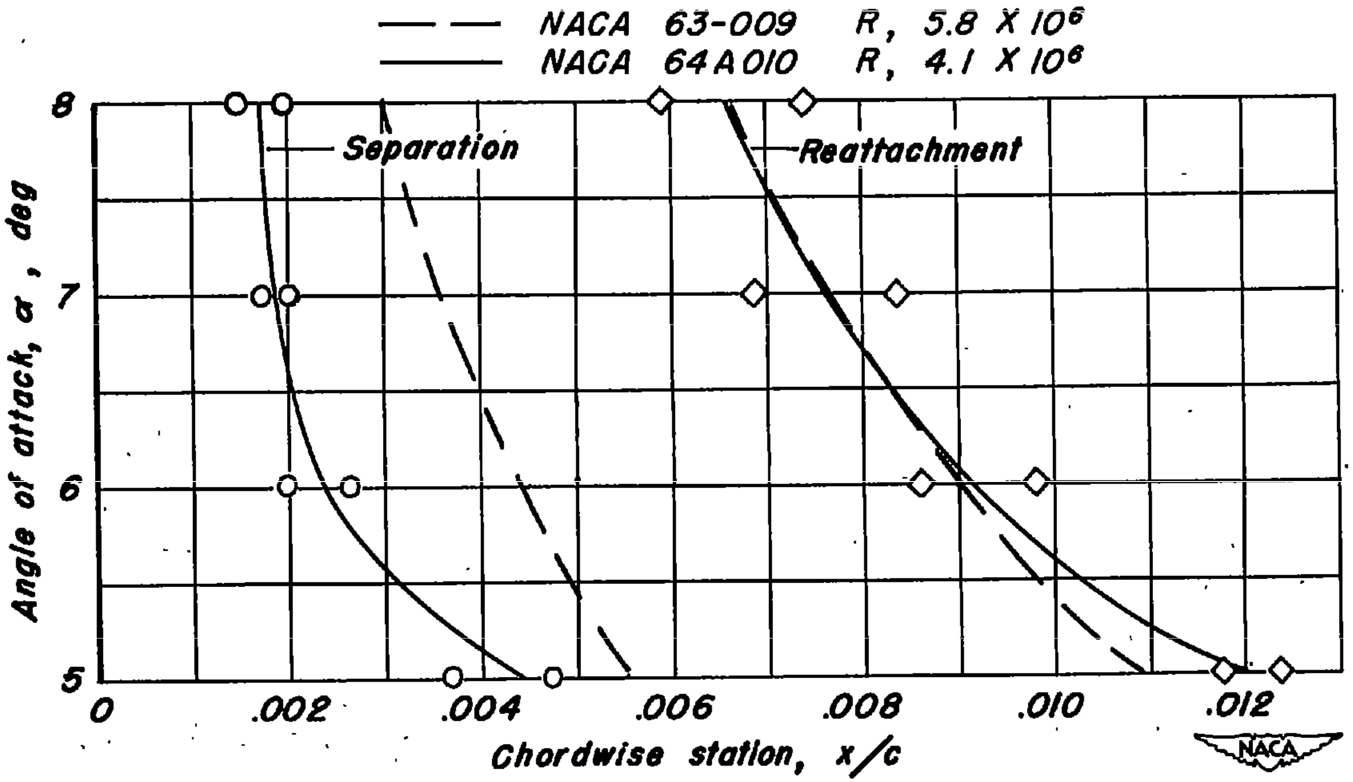

Figure 5.— Location of the region of separation as determined by the liquid-film method.

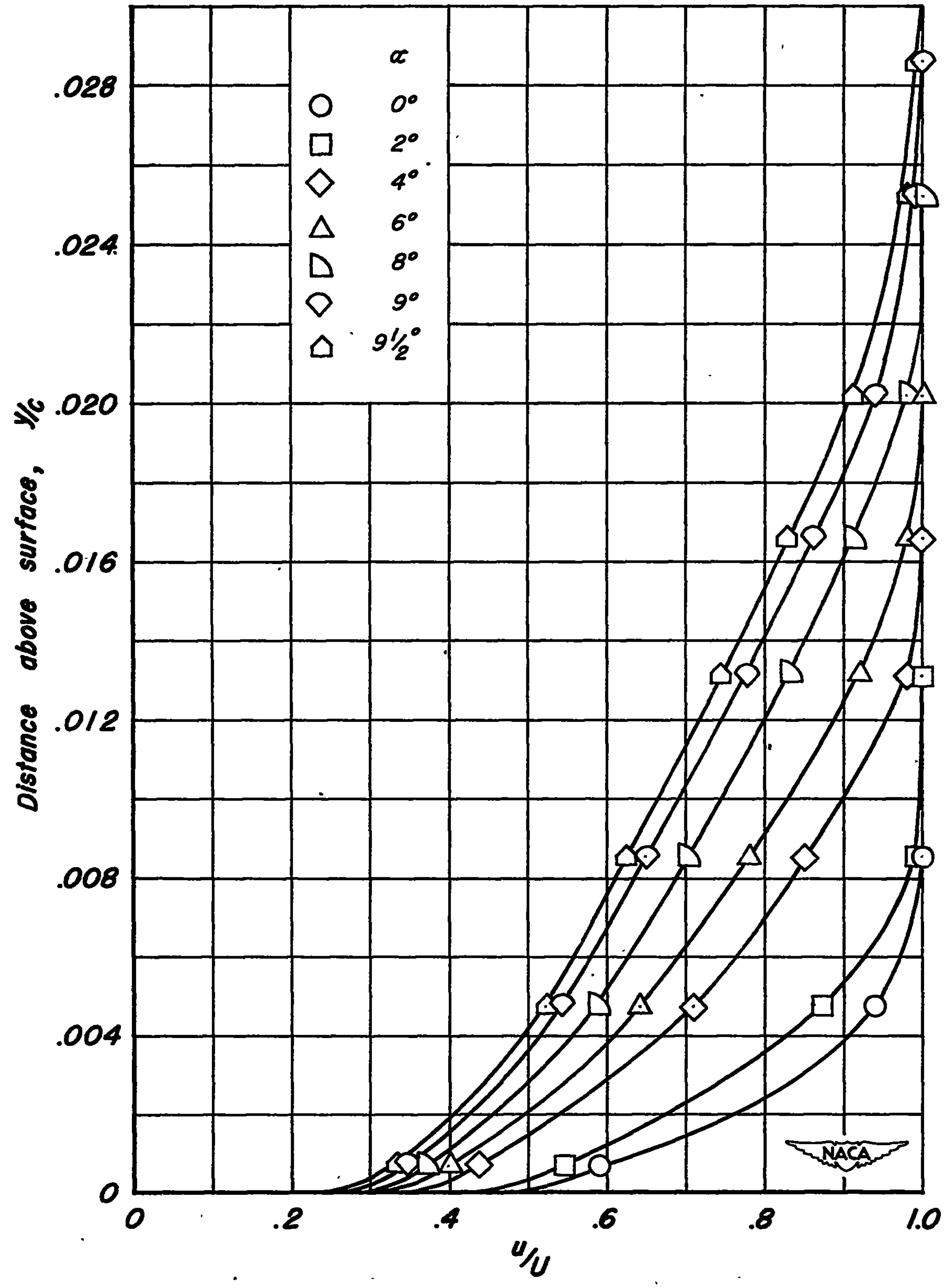

Figure 6.— Boundary-layer velocity profiles at 80 percent chord.

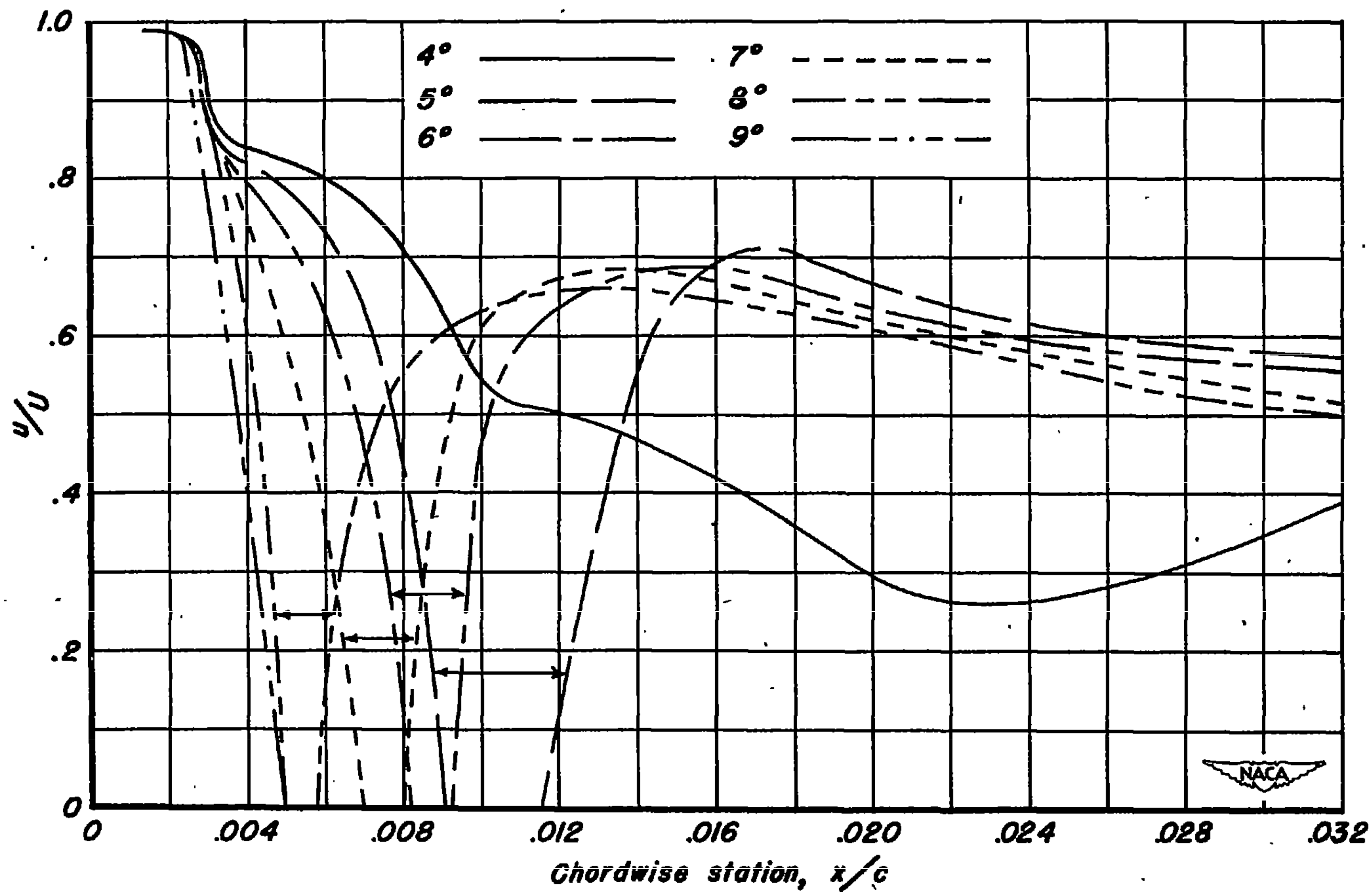

Figure 7.— Variation of velocity ratio with chordwise station as determined by surface-tube measurements.

NACA-Langley - 11-29-50 - 1275